April, 1991]

Bull. Chem. Soc. Jpn., 64, 1205—1212 (1991) 1205

ESR and Magnetic Susceptibility Studies on High-Spin Tetrahedral Cobalt(II)-Thiolate Complexes: An Approach to Rubredoxin-Type Active Sites

Kouichi Fukui, Hiroaki Ohya-Nishiguchi,* and Noboru Hirota
Department of Chemistry, Faculty of Science, Kyoto University, Sakyo-ku, Kyoto 606

(Received December 3, 1990)

Magnetic susceptibility and ESR studies on high-spin (S=3/2) tetrahedral cobalt(II)-thiolate complexes were performed for $A_2[Co(SPh)_4]$; A=Me_4N (**1a**), Et_4N (**1b**), Ph_4P (**1c**) and $(Et_4N)_2[Co(SR)_4]$; R=C_6H_4-*p*-Me (**2**), C_6H_4-*p*-Cl (**3**), C_6F_5 (**4**). It was found that the magnitude of zero-field splitting and the anisotropy of *g*-factor are exceptionally large for **1c** as $D \approx -100\,cm^{-1}$, $E \approx 0$, $g_x \approx g_y < g_z$. This parameter set shows that $Co(SPh)_4{}^{2-}$ in **1c** is strongly affected by an axial distortion. On the contrary, a rhombic distortion with moderate magnitude was found for **1a** ($D^*=6.5\,cm^{-1}$, $E/D=-0.21$) and **1b** ($D^*=5.0\,cm^{-1}$, $E/D=0.19$). The results for the other compounds are $D^*=7.0\,cm^{-1}$, $E/D=0.14$ for **2**, $D^*=12\,cm^{-1}$, $E/D=0.10$ for **3**, and $D^*=2.0\,cm^{-1}$, $E/D=0.02$ for **4**. Attempts were made to correlate the magnetic properties and the coordination geometry for **1a**—**c** by use of available X-ray data. As a result, the importance of the orientation of the thiolate ligands was confirmed.

Cobalt is an important element in bioinoganic chemistry because the Co(II) ion is frequently employed as a spectroscopic probe in metal-exchange studies of metalloproteins.[1-6] The advantage of Co(II) is derived from the sensitivity of its d-d absorptions,[7] effective magnetic moment (μ_{eff}),[8] and zero-field splitting (zfs)[9] to coordination environment around the metal ion. It has been also pointed out that the ESR spectra of high-spin Co(II) complexes are susceptible even to slight change and/or distortion of the geometry.[10-15] Many Co(II)-substituted metalloproteins, therefore, have been prepared in order to elucidate their active-site geometries with or without substrate/inhibitor by using UV-visible, MCD,[1,3,4] and ESR spectroscopies.[2-6]

Rubredoxin, which is the simplest iron-sulfur protein, contains a $Fe(SCys)_4$ site relevant to its electron-transfer function.[16] In the $Fe(SCys)_4$ site, four thiolate anions from cysteine residues are ligated to an Fe ion in a distorted tetrahedral arrangement.[17,18] Of paticular interest have been the geometric effects on the electron-transfer properties of this site. Previous molecular orbital (MO) calculations for simple models, $Fe(SR)_4{}^{-/2-}$ (R=H, CH_3), suggest that the most important geometric factor in the active site is the orientation of the thiolate ligands, rather than the tetragonal compression/elongation of the FeS_4 tetrahedron.[19,20] However, in the studies of synthetic models exemplified by $Fe(SPh)_4{}^{2-}$, the interest has been rather focused on the tetragonal distortion. In view of the sensitivity of Co(II) to coordination environment, model studies of cobalt thiolates are expected to provide valuable information concerning the relationship(s) between thiolate orientation (or other geometric factors) and electronic structure in metal thiolates. For this reason, we have chosen cobalt thiolates as a target of the present work.

The stereochemistry of metal-benzenethiolate complexes, $M(SPh)_4{}^{-/2-}$, is now well characterized through extensive X-ray studies of different metal analogs with different counter ions.[21-27] It was pointed out by Coucouvanis et al.[22] and, more explicitly, by Koch et al.,[23] that only two conformations are possible for the overall orientation of the benzenethiolates (Fig. 1): One conformation is found in $(Ph_4P)_2[M^{II}(SPh)_4]$ (M=Co, Fe, Zn, etc.).[21,22] Their S'-M-S-C tortion angles are all ca. 0° or 180°, forming a D_{2d} geometry in the idealized case. The other is found in

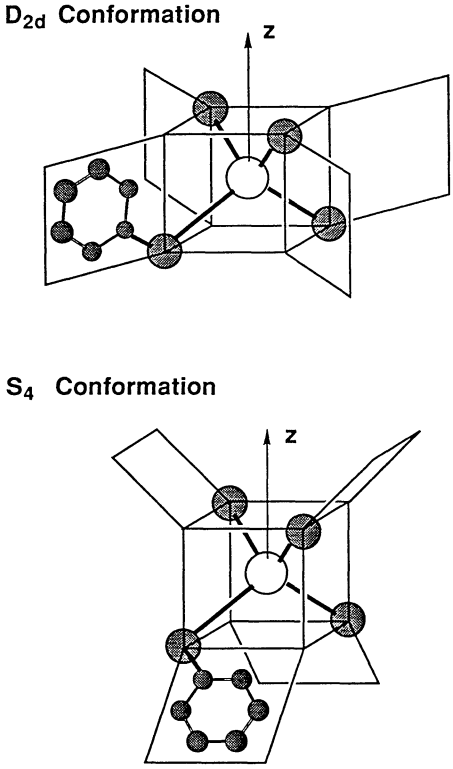

Fig. 1. Schematic drawings of the two idealized conformations for the thiolate-orientation in $M(SPh)_4{}^{-/2-}$. The phenyl rings lie in the planes standing on edges of the cubes.

$(Et_4N)[Fe^{III}(SPh)_4]$,[23] $(Me_4N)_2[M^{II}(SPh)_4]$ (M=Mn,[24] Zn[25]) and $(Et_4N)_2[M^{II}(SPh)_4]$ (M=Ni,[26] Fe (Fig. 8 in Ref. 22)). In these complexes, two of the four thiolates are rotated by ca. ±120° about the respective M–S bonds from the positions in the D_{2d} conformation. The overall symmetry is S_4 in the idealized case. Such conformational constraint is due to a combined effect of the sulfur p_π-phenyl π interactions and the ortho phenyl hydrogen-sulfur-metal interactions.[22] The active-site geometry of rubredoxin has been classified to the D_{2d} conformation,[17,18] though two of the thiolates are rotated by ca. 30° from the idealized positions.[20]

In the present paper, we report the ESR and magnetic susceptibility results of $A_2[Co(SPh)_4]$; A=Me_4N (**1a**), Et_4N (**1b**), Ph_4P (**1c**) and $(Et_4N)_2[Co(SR)_4]$; R=C_6H_4-*p*-Me (**2**), C_6H_4-*p*-Cl (**3**), C_6F_5 (**4**). Their magnetic properties (*g*-values and zfs parameters) are examined closely. The electronic structures of **1a**—**1c** are discussed based on their zfs and above-described conformational properties.

Experimental

Materials. Acetonitrile was distilled over CaH_2 and stored over molecular sieves 4A. The other reagents were used as purchased. The compounds $A_2[Co(SR)_4]$ were prepared according to a modified Dance's method[27] in vacuo or under dinitrogen atmosphere. They were obtained as emerald-green microcrystals except that **4** as blue-green powder. Their Zn analogs were prepared similarly. Magnetically diluted Zn-doped samples were obtained by recrystallization from an acetonitrile solution containing one of the Co compounds and its Zn analog in a mole ratio of Co/Zn=1% or 10%.

$A_2[Co(SPh)_4]$; A=Me_4N (1a), A=Et_4N (1b), A=Ph_4P (1c). The UV-visible spectra in CH_3CN agree well with those reported previously.[27] ^1H NMR (CD_3CN) δ=16.9 (2,m-H), −23.7 (1,p-H).[28] For **1c**, Found: C, 73.14; H, 5.02; P, 5.19%. Calcd for $CoS_4C_{72}H_{60}P_2$: C, 73.64; H, 5.15; P, 5.27%.

$(Et_4N)_2[Co(SC_6H_4$-*p*-Me$)_4]$ (2). ^1H NMR (CD_3CN) δ=17.1 (2,m-H), 27.0 (3,p-Me). Found: C, 64.02; H, 8.52; N, 3.28%. Calcd for $CoS_4C_{44}H_{68}N_2$: C, 65.07; H, 8.44; N, 3.45%.

$(Et_4N)_2[Co(SC_6H_4$-*p*-Cl$)_4]$ (3). ^1H NMR (CD_3CN) δ=17.9 (2,m-H). Found: C, 53.05; H, 6.30; N, 3.07; Cl, 15.73%. Calcd for $CoS_4C_{40}H_{56}N_2Cl_4$: C, 53.73; H, 6.31; N, 3.13; Cl, 15.87%.

$(Et_4N)_2[Co(SC_6F_5)_4]$ (4). This compound is unstable to heat, so that the temperature should be kept below 30 °C during the synthesis and stored in a refrigerator.[29] Found: C, 41.10; H, 3.61; N, 2.41; F, 32.93%. Calcd for $CoS_4C_{40}H_{40}N_2F_{20}$: C, 43.05; H, 3.59; N, 2.51; F, 34.08%.

Measurements. ESR spectra were recorded on a JEOL FE-3X spectrometer equipped with an Air Product Model LTR-3-110 Heil-Tran liquid-helium-transferring refrigerator. The microwave frequency (X-band, 9 GHz) was measured with a Takeda Riken TR5211 frequency counter. Cr(III) in MgO was used as a calibrant of the magnetic field. For the ESR measurements, each compound was examined in three forms; magnetically undiluted neat powder, magnetically diluted Zn-doped powder, and frozen MeCN solution. Magnetic susceptibility measurements were performed on a Faraday-type susceptometer over a temperature range of 1.5 K to room temperature at a magnetic field of 700 mT. Neat powder samples were used for the measurements. The temperature was measured with a thermocouple and a Ge resistor, and the magnetic field with a Hall probe. The calibrations of the temperature and the field-gradient were made using $KCr(SO_4)_2\cdot 12H_2O$ and $HgCo(NCS)_4$, respectively. Temperature-independent magnetism and μ_{eff} at room temperature, μ_{eff}(R.T.), were estimated from the least-squares fit of the data in a high-temperature region (typically 100K—room temperature) to the Curie law.

Results and Analyses

Magnetic Susceptibility. In the second column of Table 1 are listed the μ_{eff}(R.T.) values, which are all within the range for high-spin Co(II) complexes (S=3/2).[8] It is notable here that the μ_{eff}(R.T.) value of **1c** (5.0 BM) is significantly larger than the others (4.1—4.4 BM). This result, together with those given later, shows that the magnetic properties of **1c** are exceptional.

The susceptibility data of **3** and **4** are representatively shown in Fig. 2 as a μ_{eff} vs. *T* plot. The decrease of μ_{eff} at lower temperatures is attributed to thermal depopulation of the upper partner of the zero-field split levels (upper Kramers doublet). Similar temperature dependence was found for **1a**, **1b**, and **2**. The susceptibility data of **1c** is presented in Fig. 3, where a gradual decrease of μ_{eff} occurs over a wide temperature range. Although this magnetic behavior is unusual for a mononuclear complex, the ESR results of **1c** show that no exchange interaction exists between the Co ions (vide infra).

We have analyzed the variable-temperature susceptibility data by using the *S*=3/2 spin Hamiltonian;

$$H=D(S_z^2-5/4)+E(S_x^2-S_y^2)+\sum \mu g_p S_p H_p \qquad (1)$$

Here *D* and *E* denote the conventional zfs parameters and g_p (*p*=*x*,*y*,*z*) the principal *p*-component of the *g*-tensor. Some remarks should be made about the notations: (1) We take $E\geq 0$ throughout this paper, so that the sign of the rhombicity parameter (*E*/*D*)

Table 1. Results from the Variable-Temperature Magnetic Susceptibility Measurements

Compounds	μ_{eff}/BM$^{a)}$	D^*/cm$^{-1\ b)}$	g_{av}
$(Me_4N)_2[Co(SPh)_4]$ (**1a**)	4.3	6.5	2.22
$(Et_4N)_2[Co(SPh)_4]$ (**1b**)	4.4	5.0	2.27
$(Ph_4P)_2[Co(SPh)_4]$ (**1c**)$^{c)}$	5.0	100±30	$g_{x,y}$=2.25 g_z=3.13
$(Et_4N)_2[Co(SC_6H_4$-*p*-Me$)_4]$ (**2**)	4.1	7.0	2.12
$(Et_4N)_2[Co(SC_6H_4$-*p*-Cl$)_4]$ (**3**)	4.2	12±1	2.17
$(Et_4N)_2[Co(SC_6F_5)_4]$ (**4**)	4.3	2.0	2.22

a) Room-temperature values. b) The estimated errors are ±0.5 cm^{-1} when not indicated. c) Analyzed in terms of anisotropic *g*-factor.

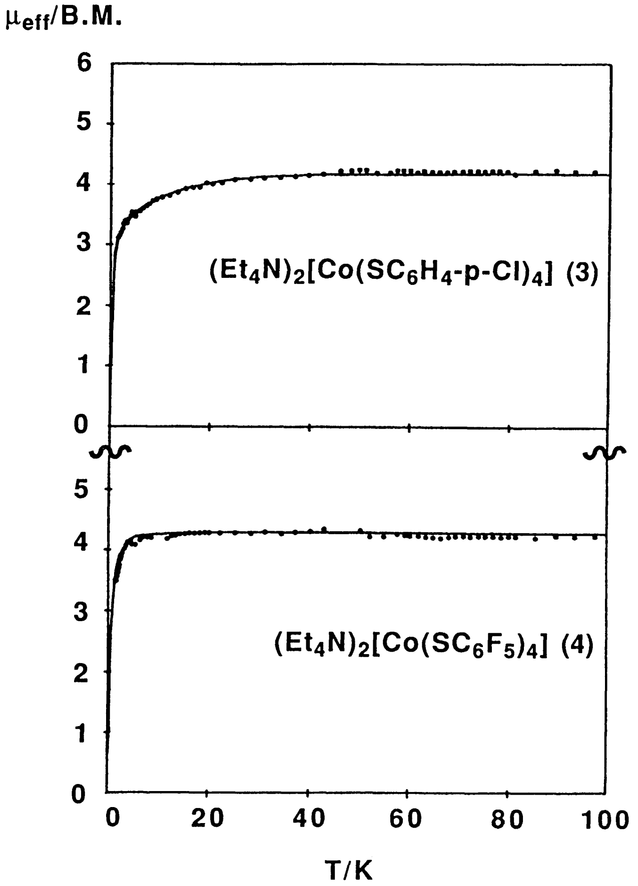

Fig. 2. Temperature dependence of μ_{eff} obtained from the neat powder samples of $(\mathrm{Et_4N})_2[\mathrm{Co(SC_6H_4}$-$p$-$\mathrm{Cl)_4}]$ (**3**) and $(\mathrm{Et_4N})_2[\mathrm{Co(SC_6F_5)_4}]$ (**4**). The solid curves represent the theoretical fits.

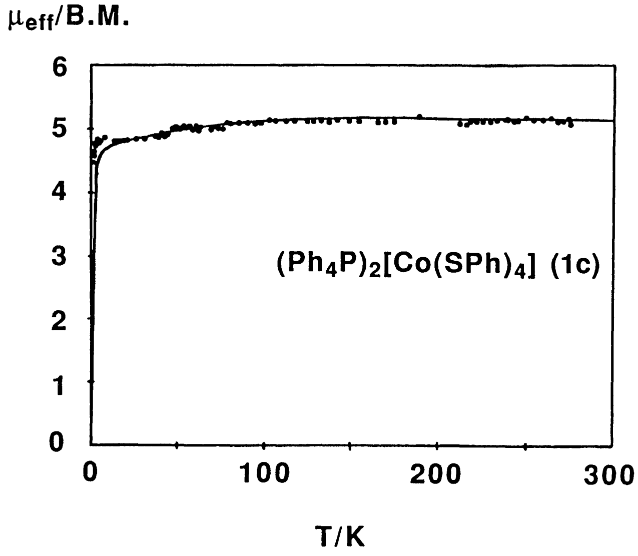

Fig. 3. Temperature dependence of μ_{eff} obtained from the neat powder sample of $(\mathrm{Ph_4P})_2[\mathrm{Co(SPh)_4}]$ (**1c**). The solid curve represents the theoretical fit, where D=-100 cm^{-1}, g_x=g_y=2.25, g_z=3.13.

always corresponds to that of D. (2) We distinguish g_p from g'_p (p=x,y,z; or p=1,2,3). g'_p is used to represent the resonant position of an ESR signal feature. The two parameters, g_p and g'_p, can be connected analytically when the Zeeman term in Eq. 1 is treated as a perturbation.[15)]

The anisotropy of g-factor is usually small in tetrahedral high-spin Co(II) complexes.[10—15,30)] Thus, in analyzing the susceptibility data, we first assumed that g-factor is isotropic (g_x=g_y=g_z=g_{av}). It is important to note that, in this case, variation of E/D has practically no effects on spatially-averaged μ_{eff}. Furthermore, g_{av} is directly connected with μ_{eff}(R.T.) as

$$\mu_{\mathrm{eff}}(\mathrm{R.T.}) = (15/4)^{1/2} g_{\mathrm{av}}. \qquad (2)$$

Hence we had only one parameter, D^*=$(D^2+3E^2)^{1/2}$, to be varied in the fitting. For **1a**, **1b**, and **2**—**4**, the best-fit curves obtained in this manner reproduce the experimental data quite satisfactorily, as shown in Fig. 2 for **3** and **4** representatively. The D^* and g_{av} values obtained for these compounds are shown in Table 1. For **1c**, however, we were not able to obtain any reasonable fits when an isotropic g-factor was assumed. The temperature-dependence behavior of μ_{eff} of **1c**, which is presented in Fig. 3, indicates that the D^* value is anomalously large, being on the order of 100 cm^{-1}. Since large zfs implies large g-anisotropy, we should go into the case of anisotropic g-factor. Hence we subsequently assumed the axial case (E=0, g_x=$g_y$$\neq$$g_z$). This assumption can be justified by the X-ray data showing an approximate $\mathrm{D_{2d}}$ structure for $\mathrm{Co(SPh)_4}^{2-}$ of **1c**.[21)] The ESR results of **1c** also suggest $E$$\approx$0, as described in Discussion. The best fit for the axial case was achieved with D=-100 ± 30 cm^{-1}, g_x=g_y=2.25, and g_z=3.13 (Fig. 3). This parameter set has a few notable features: (1) D is negative in sign and anomalously large in magnitude. The fits using positive D were always poor, and resulted in unreasonable values (i.e. g_z=0) at best. (2) g_z is very large while g_x and g_y are comparable to g_{av} of the other compounds. (3) The relation; g_x, g_y<g_z, is consistent with the negative sign of D, and its large anisotropy also with the large magnitude of D. Finally attempted were the analyses including rhombicity ($E$$\neq$0, $g_x$$\neq$$g_y$), where, unfortunately, we were not able to determine the best fit uniquely. Although many sets of parameters gave comparably good fits in this case, the above features still held for the sets. Consequently the above features must exist in the magnetic properties of **1c**.

ESR. It was found that the neat powder samples commonly exhibit broad ESR spectra even at 4.2 K. These results are due to dipolar interactions among neighboring Co ions. The dipolar interactions, as well as intermolecular exchange interactions, can be reduced by doping the compounds in diamagnetic crystals. Sharpened spectra were thus obtained from

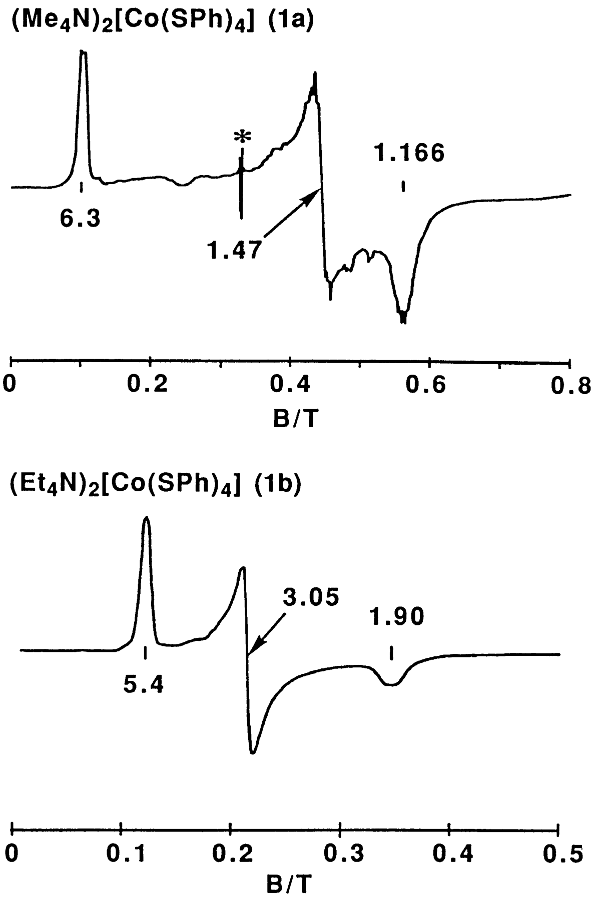

Fig. 4. ESR spectra of the Zn-doped powder samples (Co/Zn=1%) of $(Me_4N)_2[Co(SPh)_4]$ (**1a**) and $(Et_4N)_2[Co(SPh)_4]$ (**1b**) measured at 4.2 K. The signals marked with * are from a radical impurity and Cr(III) in MgO used as a *g*-value marker.

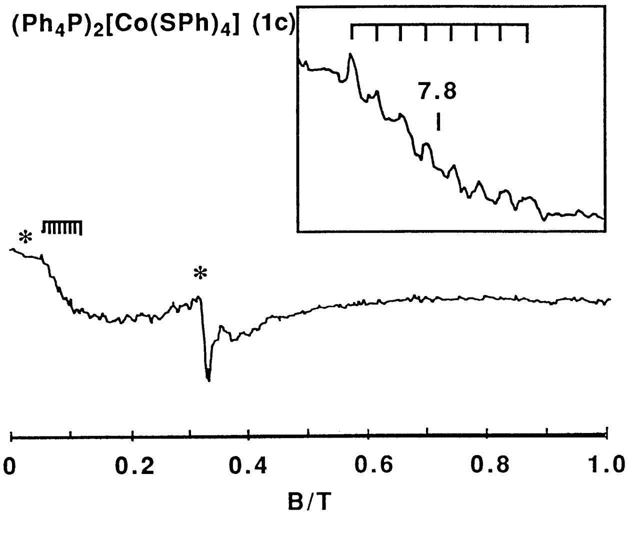

Fig. 5. ESR spectrum of the Zn-doped powder sample (Co/Zn=10%) of $(Ph_4P)_2[Co(SPh)_4]$ (**1c**): Conditions Temperature, 4.2 K; Sample amount, 30 μmol; Power 1 mW; Amplitude, 1.25×1000; Modulation, 10 G at 100 kHz. The signals marked with * are due to impurities. The g'=7.8 signal is enlarged in the inset.

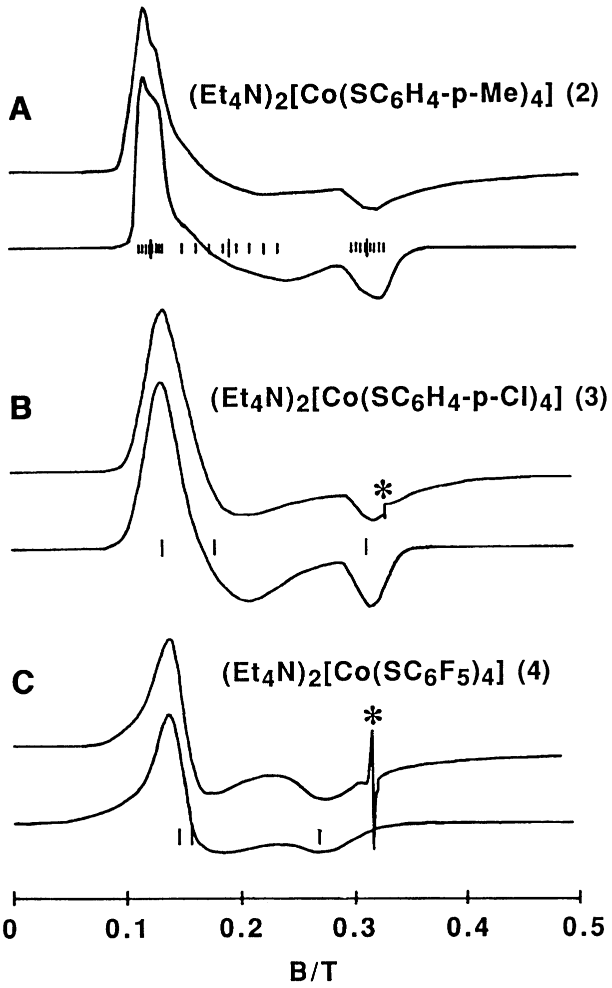

Fig. 6. ESR spectra of the Zn-doped powder samples (Co/Zn=1%) of $(Et_4N)_2[Co(SC_6H_4\text{-}p\text{-}Me)_4]$ (**2**), $(Et_4N)_2[Co(SC_6H_4\text{-}p\text{-}Cl)_4]$ (**3**), and $(Et_4N)_2[Co(SC_6F_5)_4]$ (**4**) obtained at 4.2 K. The lower spectrum for each is the result from the computer simulation. The signals marked with * are from Cr(III) in MgO (B) and from a radical impurity (C).

the Zn-doped samples as shown in Fig. 4 for **1a** and **1b**, in Fig. 5 for **1c**, and in Fig. 6 for **2**—**4**. The sharpening of the spectra was especially drastic for **1a** and **1b**. The principal g'-values obtained from the Zn-doped spectra are summarized in Table 2. For **1b**, **1c**, and **2**—**4**, the Zn-doped powder spectra are practically identical with the corresponding neat powder spectra excepting the difference in line width. This suggests that the geometric distortions are not altered appreciably by the Zn-doping. (Especially **1c** is known to be isomorphous and isostructural to the Zn analog.[21]) For **1a**, however, the two spectra are slightly different, although this difference does not seem to be so important.[31] Thus in the two states the geometric distortions of **1a** are not exactly the same, but still essentially similar.

In the Zn-doped spectrum of **1a**, each signal feature contains a partially resolved hyperfine structure due to

Table 2. Results from the ESR Measurements of the Zn-Doped Powder Samples at 4.2 K

Compounds	g'-Values			hfcc/mT[a)]			E/D[b)]	g_{gv}
	g'_1	g'_2	g'_3	A_1	A_2	A_3		
$(Me_4N)_2[Co(SPh)_4]$ (**1a**)	6.3	1.47	1.166	0.8	4.0	4.4	−0.21	2.19
$(Et_4N)_2[Co(SPh)_4]$ (**1b**)	5.4	3.05	1.90			2*	0.19	2.16
$(Ph_4P)_2[Co(SPh)_4]$ (**1c**)	7.8[c)]			9.2[c)]			−0	
$(Et_4N)_2[Co(SC_6H_4\text{-}p\text{-}Me)_4]$ (**2**)	5.1	3.3	2.04	3*	12*	4*	0.14	2.14
$(Et_4N)_2[Co(SC_6H_4\text{-}p\text{-}Cl)_4]$ (**3**)	4.8	3.6	2.08				0.10	2.12
$(Et_4N)_2[Co(SC_6F_5)_4]$ (**4**)	4.3	4.0	2.35				0.02	2.11

a) The values marked with * are from the simulations. b) The estimated errors are about ±0.02. The negative sign means negative D value. c) Very weak.

^{59}Co ($I=7/2$). The coupling constants are A/mT=0.8 at $g'=6.3$, 4.0 at $g'=1.47$, and 4.4 at $g'=1.166$. As for **1b**, we did not observe any resolved hyperfine splittings. However, the line shape of the $g'=1.90$ feature is indicative of unresolved structure of A≈2 mT (Fig. 4).

No apparent ESR signals were obtained from **1c** despite that we measured some forms of samples from different sources each. Both the Zn-doped (Co/Zn=10%) and the neat powder samples of **1c** exhibit only an incomplete and extremely weak signal up to 1.0 T even at 4.2 K. This signal is centered at $g'=7.8$ with a resolved hyperfine structure of $A=9.2$ mT, although the signal was too weak to be detected clearly (Fig. 5). Under the same conditions, the low-field components of the other compounds gave 100—1000 times the intensity of the $g'=7.8$ signal. No signal has been obtained from the Co/Zn=1% sample, which is however consistent with the extraordinary weakness of the $g'=7.8$ signal. Although uncertainty remains as to whether the $g'=7.8$ signal is attributable to **1c**, it is at least clear that the ESR signal of this compound is extremely weak or even can not be observed. Weakness (or absence) of ESR signals is often attributed to intermolecular exchange interaction. However, the fact that weak (or no) signal is invariably observed from the three different forms shows that this is not the case. Additionally, the crystallographic data of the X-ray isomorphous Fe analog show that the nearest-neighboring metal ion sites are separated sufficiently by 10 Å. The origin of the weakness is discussed later.

The ESR spectra of Zn-doped **2**, **3**, and **4** are relatively broad, so that we simulated the spectra to estimate the principal g'-values (Fig. 6). The simulations are based on the $S'=1/2$ effective spin Hamiltonian using the gaussian-type lineshape function.[5)] The compound **2** gives a characteristic signal shape from 0.1 to 0.2 T. This shape can only be reproduced when a fairly large but unresolved hyperfine splitting is assigned to the principal $g'=3.3$ component. On the other hand, the spectra of **3** and **4** show no evidence for hyperfine splittings, so that hyperfine interaction was neglected in the simulations of these spectra.

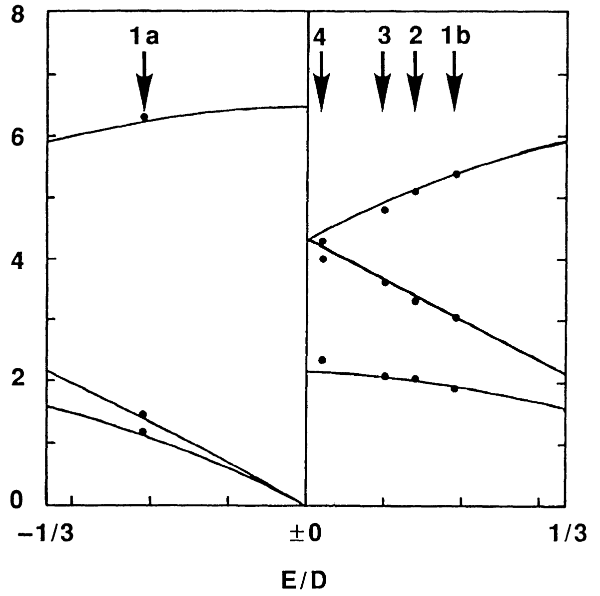

Fig. 7. Theoretical curves of g'-values versus E/D accompanied by the experimental results from the Zn-doped powder samples.

In contrast to the low-temperature behavior of μ_{eff}, g'_p does not depend on D^* but only on g_p and E/D when $D^* \gg h\nu=0.3$ cm^{-1}. The variation of g'_p vs. E/D is graphed in Fig. 7 for the transition within the lower Kramers doublet, together with the experimental values from the Zn-doped powder spectra. Since the intensities of the observed signals all decrease with increasing temperatures above 4.2 K, the signals are assigned to arise from the lower doublets. Based on these assignments and approximation of isotropic g-factor, we have estimated E/D and g_{av} (Table 2). These g_{av} values are in good agreement with those obtained from the susceptibility results.

The ESR spectra obtained from the frozen solution samples are less informative. All the compounds including **1c** exhibit similar spectra, which consist of broad features at $g'\approx4$ and ≈2. However, the observation of such broad spectra is not surprising. In solution, no uniformity is anticipated among the conformations or distortions of the complexes, to which the ESR spectrum is sensitive as typically demonstrated by the powder spectra of **1a**—**c**.

Discussion

Magnetic Properties of 1c. We have estimated the zfs parameters, D^* and E/D, from the susceptibility and ESR results, respectively, for **1a**, **1b**, and **2**—**4**. For **1c**, while it is now clear from the susceptibility data that $D^* \approx 100$ cm^{-1} and $D<0$, E/D still remains ambiguous. The ESR signals from the powder samples of **1c** are always too weak to allow a definite estimate of E/D. However, the extraordinary weakness is indicative of a negligibly small E value. When $E/D=-0$ (here '-0' means $E=0$ and $D<0$ simultaneously), the lower Kramers doublet consists of pure $S_z=\pm 3/2$ states. Then the transition within this doublet is forbidden and no (or very weak) ESR signal is expected. Indeed the transition within the upper doublet is alternatively allowed, but large zfs as in **1c** makes it difficult to detect this transition because of insufficient thermal distribution to this doublet. A literature example for this situation is bis(*N*-*t*-butylpyrrolecarbaldimino)cobalt(II),[13,15] which was reported to be ESR silent and assigned as $E/D=-0$. On the other hand, when E is not negligible, the ground $S_z=\pm 3/2$ states are mixed with the $S_z=\pm 1/2$ ones and, hence the transition gains some intensity. This is the very case for Zn-doped **1a** ($E/D=-0.21$), which exhibits enough intense ESR spectrum. We therefore conclude that $E/D=-0$ is most likely for **1c**. We also point out that the g'_z value predicted for $E/D=-0$ ($g'_z=3g_z=9.4$) can be compared with the observed value of $g'=7.8$.

***g*-Factor.** For high-spin tetrahedral Co(II) complexes, the deviation of g-values from the free-electron value arises mainly from the interaction between the ground $^4A_2$ and the lowest excited $^4T_2$ states through the spin-orbit coupling. Thus g_{av} is expressed as[30]

$$g_{av} \approx 2 - 8k^2\lambda_0/\Delta_t, \tag{3}$$

where k represents the orbital-reduction factor, λ_0 the spin-orbit coupling constant for the free ion (-178 cm^{-1}), and Δ_t the energy separation between the e and t$_2$ orbitals (4030 cm^{-1}).[32] By using the most reliable values of $g_{av}=2.16$—2.19, which are from the ESR results of Zn-doped **1a** and **1b**, we obtain $k=0.67$—0.73. This k value is remarkably small compared with those of other tetrahedral Co(II) complexes; for example, $k=0.8$ for a CoN$_4$ chromophore,[14] $k=0.9$ for a CoO$_4$ chromophore,[33] and $k=0.92$ for $CoCl_4^{2-}$.[34] This remarkable reduction of k, together with that of the Racah parameter B,[32] shows a highly covalent character of the Co-S bondings. Such high covalency was also reported for Fe-S bondings.[35]

The remarkable g-anisotropy in **1c**, together with the large zfs, suggests that the electronic structure is deviated extremely from that under T$_d$ symmetry. This deviation must contain a remarkably low excitation energy of the z-component of $^4T_2$, as is evident from the large g_z value. This excitation energy could be estimated by using a modified version of Eq. 3 if the obtained g-values were sufficiently reliable. However, unfortunately, the g-values of **1c** are less reliable because they were obtained only from powder susceptibility data. Further ESR and susceptibility studies on **1c** are now in progress by using single crystals.

ZFS Parameters. Previously Makinen et al.[9] reported that D^* can be a good measure of the coordination number for high-spin Co(II) complexes: The D^* value should be in the range of 0—6.5 cm^{-1} for tetrahedral ones, 10—25 cm^{-1} for pentacoordinate ones, and larger than 25 cm^{-1} for octahedral ones. If we followed this criterion, we could assign **3** as a pentacoordinate complex, and **1c** as an octahedral one. However, these assignments are unreasonable, contradicting the X-ray data which undoubtedly show a tetrahedral geometry for **1c**. As has been pointed out elsewhere,[5] the criterion by Makinen et al. is not so strict. This is because the complexes which they treated are rather simple and possess mild distortions in the coordination geometries.

Interestingly, the D^* values of **1a**, **1b**, and **2**, though they are much smaller than that of **1c**, can be presumed to be *large* (when compared with simple complexes) according to the criterion. It is of great interest to examine whether the *large* D^* values can be interpreted in terms of the tetragonal compression/elongation, which has been supposed to be an important geometric factor in metal-thiolate complexes.[21—27] There have been several theoretical studies concerning the relationship between zfs and the magnitude of the tetragonal distortion. For example, according to the equation given by Fukui et al. (Eq. 25 in Ref. 36), the contribution to D from the tetragonal distortion, D_{tet}, for the CoS$_4$ cores is expressed as

$$D_{tet}/\mathrm{cm}^{-1} \approx 0.57(\theta/\mathrm{deg} - 109.47). \tag{4}$$

Here we have used $\Delta_t=4030$ cm^{-1}, $\lambda=k\lambda_0\approx-125$ cm^{-1}. θ is the S-Co-S′ angle whose bisector coincides with the tetragonal axis. Equation 4 shows that, as θ varies in a range plausible for the CoS$_4$ cores (95°—120°),[21] the D_{tet} value varies from -8 to 6 cm^{-1}. Thus, for **1a**, **1b**, and **2**, it seems reasonable to attribute the *large* zfs (in the sense of Makinen's criterion) to large tetragonal distortion of the CoS$_4$ core. This situation further leads to another important conclusion that the zfs in **1c** is too large to be interpreted in terms of the tetragonal distortion.

Magnetic Properties and Thiolate Orientation. Since **1a**, **1b**, and **1c** have the identical anion complex, the wide variety among their magnetic properties provides a good example for the sensitivity of Co(II) complexes to changes in coordination environment. This wide variety also provides an opportunity to investigate the relationship between the geometric distortion and the electronic structure in metal-thiolate complexes. The X-ray molecular structure of **1c** was reported previously, showing the D_{2d} conformation for the overall orientation of the SPh^- ligands (Fig. 1).[21] Although no X-ray data are available for the other compounds, the Zn analog of **1a**, $(Me_4N)_2[Zn(SPh)_4]$ (**5**), has been studied by X-ray crystallography.[25] Because the ESR spectrum of Zn-doped **1a** is reasonably sharp, **1a** is expected to have the same geometry as **5** at least in the Zn-doped sample. It is known that **5** has the S_4 conformation for the overall thiolate orientation (Fig. 1). Notably the S–M–S′ angles are very similar between **1c** and **5**. The observation of the remarkably different magnetic properties between **1c** and Zn-doped **1a**, therefore, confirms the importance of the thiolate orientation in metal-thiolate complexes.

In the D_{2d} conformation, the phenyl rings lie in the same direction with respect to the z-axis. Thus the sulfur p_π-orbitals, which are in conjugation with the corresponding phenyl π-orbitals, are all perpendicular to the z-axis. This coordination mode will produce a strong axial ligand field and, hence give large and axial zfs. This expectation is consistent with the observed zfs for **1c**. In the S_4 conformation, on the other hand, the sulfur p_π-orbitals are no more in phase, or interact with a specific metal d-orbital. Little contribution is therefore expected toward zfs from the ligand field due to the sulfur p_π-orbltals. This explains the relatively small D^* value of **1a**.[37] It seems from Eq. 4 that zfs under the S_4 conformation is rather dominated by the tetragonal distortion and some rhombic distortion, where the latter breaks the strict S_4 symmetry and generates the E parameter. Similar explanation can be adopted to the zfs of **1b**, whose Fe(II)[22] and Ni(II)[26] analogs also have the S_4 conformation.

Based on the above consideration, we infer that **2**, **3**, and **4** have the S_4 conformation because their D^* values are rather small.[38] The slightly larger D^* value of **3** is probably due to a minor difference in the thiolate orientation. Here it is worth noting that the ortho-substitutions in **4** may lead to another type of thiolate conformation as found in Fe(2,3,5,6-tetramethylbenzenethiolate)$_4^-$. In this complex, steric hindrance due to the ortho methyl groups prevents the Fe–S–C and phenyl-ring planes from being coplanar. They are rather perpendicular to each other, though the overall geometry retains S_4 symmetry.[39] Recently the electronic structure of this complex was examined closely.[35]

Finally we turn our attention to the active-site geometry of rubredoxin. The ESR spectrum of oxidized rubredoxin is featured by an isotropic $g'=4.3$ feature,[40] which is indicative of an extremely rhombic geometry ($E/D=1/3$) around the Fe ion. Interestingly, nearly extreme rhombicity is found in the zfs of **1a** and **1b** (See Table 2). At the moment it is not clear whether the extreme rhombicity is only an accidental phenomenon or not. Nevertheless, it is notable that the appearance of the extreme rhombicity is not consistent with the D_{2d} conformation proposed so far for the active-site geometry of rubredoxin. This situation implies the importance of the seemingly irrelevant distortion; the rotations of two thiolates by ca. 30° from the idealized positions. The importance of this distortion was previously pointed out by Ueyama et al. from extended Hückel MO calculations.[20] Unfortunately it seems that neither ESR nor magnetic susceptibility study has been performed for Co(II)-substituted rubredoxin, though the Co(II)-substitution has been accomplished.[1] However, the present work arouses the interest in the magnetic properties of Co(II)-substituted rubredoxin, and other Co(II)-substituted metalloproteins possessing rubredoxin-type active sites. Such metal-exchange approaches will provide further insight into the geometric effects on the electronic structure and the electron-transfer properties of the sites.

We thank Dr. Ryuichi Imamura for the measurements of the NMR spectra. This work is partially supported by the Grant-in-Aid for Sientific Research No. 01470050 from the Ministry of Education, Science and Culture.

References

1) S. W. May and J.-Y. Kuo, *Biochemistry*, **17**, 3333 (1978).

2) L. C. Kuo and M. W. Makinen, *J. Am. Chem. Soc.*, **107**, 5255 (1985).

3) R. Bicknell, A. Schäffer, S. G. Waley, and D. S. Auld, *Biochemistry*, **25**, 7208 (1986).

4) M. Good and M. Vask, *Biochemistry*, **25**, 3328 (1986).

5) R. A. Martinelli, G. R. Hanson, J. S. Thompson, B. Holmquist, J. R. Pilbrow, D. S. Auld, and B. L. Vallee, *Biochemistry*, **28**, 2251 (1989). References concerning the theoretical foundation of the ESR simulation are cited therein. The difference between their simulation and ours is that theirs includes the M_I dependence of line widths while ours not

6) S. Dahlin, B. Reinhammar, and Ånström, *Biochemistry*, **28**, 7224 (1989).

7) W. D. Behnke and B. L. Vallee, *Proc. Natl. Acad. Sci. U.S.A.*, **69**, 2442 (1972).

8) L. Sacconi and R. Morassi, *J. Chem. Soc. A*, **1970**, 575.

9) M. W. Makinen, L. C. Kuo, M. B. Yim, G. B. Wells, J. M. Fukuyama, and J. E. Kim, *J. Am. Chem. Soc.*, **107**, 5245 (1985).

10) L. J. Guggenberger, C. T. Prewitt, P. Meakin, S. Trofimenko, and J. P. Jesson, *Inorg. Chem.*, **12**, 508 (1973).

11) A. Bencini and D. Gatteschi, *Inorg. Chem.*, **16**, 2141 (1977).

12) A. Bencini, C. Benelli, D. Gatteschi, and C. Zanchini, *Inorg. Chem.*, **18**, 2137 (1979); *ibid.*, **18**, 2526 (1979); *ibid.*, **19**, 1301 (1980); *ibid.*, **19**, 3839 (1980).

13) A. Bencini and D. Gatteschi, *Transition Met. Chem. (N.Y.)*, **8**, 1 (1982).

14) L. Banci, C. Benelli, D. Gatteschi, and F. Mani, *Inorg.*

Chem., **21**, 1133 (1982).

15) H. Drulis, K. Dyrek, K. P. Hoffmann, S. K. Hoffmann, and A. Weselucha-Birczynska, *Inorg. Chem.*, **14**, 4009 (1985).

16) A. J. Thomson, "Metallproteins," Part 1, ed by P. M. Harrison, Macmillan Press, Hampshire (1985).

17) K. D. Watenpaugh, L. C. Sieker, and L. H. Jensen, *J. Mol. Biol.*, **131**, 509 (1979).

18) M. Frey, L. Sieker, F. Paya, R. Haser, M. Bruschi, G. Pepe, and J. LeGall, *J. Mol. Biol.*, **197**, 525 (1987).

19) R. A. Bair and W. A. Goddard III, *J. Am. Chem. Soc.*, **100**, 5669 (1978); L. Noodleman, J. G. Norman, Jr., J. H. Osborne, A. Aizman, and D. A. Case, *J. Am Chem. Soc.*, **107**, 3418 (1985).

20) N. Ueyama, T. Sugawara, K. Tatsumi, and A. Nakamura, *Inorg. Chem.*, **26**, 1978 (1987).

21) D. Swenson, N. C. Baenzigar, and D. Coucouvanis, *J. Am. Chem. Soc.*, **100**, 1932 (1978).

22) D. Coucouvanis, D. Swenson, N. C. Baenzigar, C. Murphy, D. G. Holah, N. Sfarnas, A. Simopoulos, and A. Kostikas, *J. Am. Chem. Soc.*, **103**, 3350 (1981).

23) S. A. Koch, L. E. Maelia, and M. Millar, *J. Am. Chem. Soc.*, **105**, 5944 (1983).

24) T. Sugawara, N. Ueyama, A. Nakamura, and N. Yasuoka, The 39th Symposium on Coordination Chemistry of Japan, Mito, 1989, Abstr., No. 3D05, p. 671.

25) N. Ueyama, T. Sugawara, N. Sasaki, A. Nakamura, S. Yamashita, Y. Wakatsuki, H. Yamazaki, and N. Yasuoka, *Inorg. Chem.*, **27**, 741 (1988).

26) T. Yamamura, H. Miyamae, Y. Katayama, and Y. Sasaki, *Chem. Lett.*, **1985**, 269.

27) I. G. Dance, *J. Am. Chem, Soc.*, **101**, 6264 (1979).

28) a) The signs are positive for the chemical shifts downfield of Me_4Si peak, and are negative for those upfield. b) Unfortunately no ortho-hydrogen peaks were observed in a range of −30—30 ppm. For $Fe(SPh)_4^{2-}$, the *o*-H peak is very broad because of the vicinity to the paramagnetic Fe ion. Thus it is likely that the *o*-H peaks of the cobalt thiolates are also broad and difficult to detect. (K. S. Hagen, J. G. Reynolds, and R. H. Holm, *J. Am. Chem. Soc.*, **103**, 4054 (1981)).

29) B. A. Averill, T. Herskovitz, R. H. Holm, and J. A. Ibers, *J. Am. Chem. Soc.*, **95**, 3523 (1973).

30) J. S. Griffith, "The Theory of Transition Metal Ions," Cambridge University Press, Cambridge (1961).

31) The neat powder sample of **1a** exhibits broad features at $g_1'\approx6$, $g_2'\approx g_3'\approx2$ ($E/D\approx1/3$). It is known that an exact isomorphism does not occur between **1a**[27] and its Zn analog.[25]

32) R. W. Lane, J. A. Ibers, R. B. Frankel, G. C. Papaefthymiou, and R. H. Holm, *J. Am. Soc.*, **99**, 84 (1977).

33) K. Kojima, J. Matsuda, N. Kojima, T. Ban, and I. Tsujikawa, *Bull. Chem. Soc. Jpn.*, **60**, 3213 (1987).

34) W. DeW. Horrocks, Jr. and D. A. Burlone, *J.Am. Chem. Soc.*, **98**, 6512 (1976).

35) J. C. Deaton, M. S. Gebhard, S. A. Koch, M. Millar, and E. I. Solomon, *J. Am. Chem. Soc.*, **110**, 6241 (1988); M. S. Gebhard, J. C. Deaton, S. A. Koch, M. Millar, and E. I. Solomon, *ibid.*, **112**, 2217 (1990).

36) K. Fukui, H. Ohya-Nishiguchi, and N. Hirota, *Mol. Phys.*, **71**, 1269 (1990).

37) Stricktly speaking, the D^* value of Zn-doped **1a** is not known. However, the ESR spectrum of the Zn-doped powder sample was well analyzed by using isotropic *g*-factor. This fact indicates that the D^* value is not so large, either.

38) A preliminary single crystal X-ray analysis of **3** confirms the S_4 conformation for this compound: $(Et_4N)_2$-$[Co(SC_6H_4\text{-}p\text{-}Cl)_4]$; $P2_1/c$, a=12.388, b=12.251, c=59.850 Å, β=95.85°, V=9035.9 Å^3, Z=8. The complete structure determination, however, has been hampered because the lattice parameter c is too large. We thank Dr. Hideki Masuda (Institute for Molecular Science) for the X-ray analysis.

39) M. Millar, J. F. Lee, S. A. Koch, and R. Fikar, *Inorg. Chem.*, **21**, 4105 (1982).

40) K. K. Rao, M. C. Evans, R. Cammack, D. O. Hall, C. L. Thompson, P. J. Jackson, and C. E. Johnson, *Biochem. J.*, **129**, 1063 (1972).
